

A Study of FSS in Terahertz Range for Polarization Modulation Purpose

Kejian Chen, Zhou Li, Jingjing Liu, Ruixin Duan, Yiqi Wang, Wen Zhang, Bin Cai, Lin Chen, and Yiming Zhu

Abstract—A polarization sensitive frequency selective surface (FSS) composed of connected electric LC resonators is proposed as the terahertz wave filter. The experimental results match the simulation results well and show that the FSS has good capability of polarization control and wavelength selection. The tunability of FSS is also studied by investigating the relation between the conductivity of the joint area of bent-lines and the resonant peak position/strength. Such a device can be applied as a flexible polarization modulator.

Index Terms—Spectroscopy, terahertz, optoelectronics, filters, FSS.

I. INTRODUCTION

WITH the development of THz emitters and detectors, more and more THz functional components are being studied to promote the performance of THz spectroscopy/imaging system. In this letter, we focus on one key component: THz wave filter. It can be fabricated by utilizing the polarization dependent FSSs. Originally FSS is widely used in microwave as a filter for freely propagating waves [1] and now, it has become a promising candidate for the high performance THz filters [2] and THz wave plates owing to its ‘openness’. FSS is a two-dimensional periodic array of resonating metallic-dielectric units, which used to be adopted as filtering elements for free-space radiation [3].

Manuscript received March 31, 2013; revised May 17, 2013 and June 13, 2013; accepted June 24, 2013. Date of publication June 27, 2013; date of current version July 31, 2013. This work was supported in part by the Leading Academic Discipline Project of Shanghai Municipal Government under Grant S30502, in part by the Shanghai Young College Teacher Develop funding schemes under Grant slg11006, in part by the Institute of Shanghai Industrial Research on Optical, Mechanical and Electronic Integration Technology under Grant 5312302001(02), in part by the National Natural Science Foundation of China under Grants 61205095, 11174207, 61138001, and 61007059, in part by the Major National Development Project of Scientific Instrument and Equipment under Grants 2011YQ150021 and 2012YQ140005, in part by the Key Scientific and Technological Project of Science and Technology Commission of Shanghai Municipality under Grant 11DZ1110800, in part by the Shanghai Basic Research Program under Grant 11ZR1425000, and in part by the Basic Research Key Project under Grant 12JC1407100.

K. Chen, Z. Li, R. Duan, Y. Wang, W. Zhang, B. Cai, L. Chen, and Y. Zhu are with the Shanghai Key Lab of Modern Optical System, Engineering Research Center of Optical Instrument and System, the Ministry of Education, Institute of Optical-Electrical Information, University of Shanghai for Science and Technology, Shanghai 200093, China (e-mail: kjchen@usst.edu.cn; zhouzhou0616@hotmail.com; duanruixin1991@gmail.com; wyq468@gmail.com; zhangw2009summer@gmail.com; bullcai@gmail.com; linchen@usst.edu.cn; ymzhu@usst.edu.cn).

J. Liu is with the Department of Electronic Engineering and Centre for Advanced Research in Photonics, The Chinese University of Hong Kong, Hong Kong (e-mail: jliu@ee.cuhk.edu.hk).

Color versions of one or more of the figures in this letter are available online at <http://ieeexplore.ieee.org>.

Digital Object Identifier 10.1109/LPT.2013.2271584

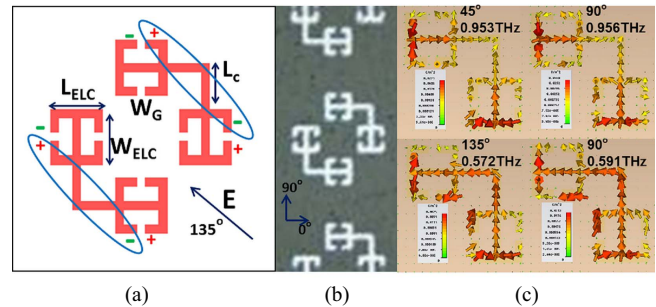


Fig. 1. (a) A unit of the FSS sample. (b) The photo of the real FSS sample. (c) The surface current of FSS sample.

The basic resonating structures of the FSSs include splitting (SRRs) [4], electric LC (ELC) [5], cut wire, slots, bent-lines [6], cross lines etc. The ‘openness’ of FSS on geometry make it easy to integrate different functional structures into a chip to realize multi-functional resonating. In this letter, a switchable polarization sensitive FSS THz filter is designed and fabricated on a flexible substrate. Its filtering properties were investigated with both simulations and experiments and the results matched well. Furthermore, based on the results, several potential applications of the device were also proposed.

II. THE STRUCTURE OF THE DEVICE AND ITS FABRICATION

The structure of the resonating units of the FSS filter is shown in Fig. 1(a), where each unit comprises 4 square ELC structures and 2 connecting bent-lines. To enable such device to work in the THz range, the unit size of the FSS is set to be $200\ \mu\text{m}$ (Wood’s Anomaly appears around 1.3 THz), and the widths of all the lines are set to be $7\ \mu\text{m}$. The side length of the ELC resonator square [7] is $41\ \mu\text{m}$ ($L_{\text{ELC}} = W_{\text{ELC}}$), and the length of the stripe line (one arm of the bent-line structure) is $74\ \mu\text{m}$ ($W_{\text{ELC}} (41\ \mu\text{m}) + L_c (33\ \mu\text{m})$). The FSS is polarization dependent with the connecting bent-lines. We defined the polarization angle as illustrated in Fig. 1(a).

The fabrication for the FSS device is taken on a Polyimide (PI) substrate, which is a low cost but among best choices for THz passive devices fabrication and would be removed from Si wafer after fabrication with the normal semiconductor processing technology. In this letter, the thicknesses of the PI substrate and the copper layer were $21\ \mu\text{m}$ and $2\ \mu\text{m}$, respectively. A photo of the fabricated device is given in Fig. 1(b). The whole size of the FSS device is $1\ \text{cm} \times 1\ \text{cm}$. The fabricated FSS device is mounted on a metal holder with a square hole at its center and the size a little smaller than the

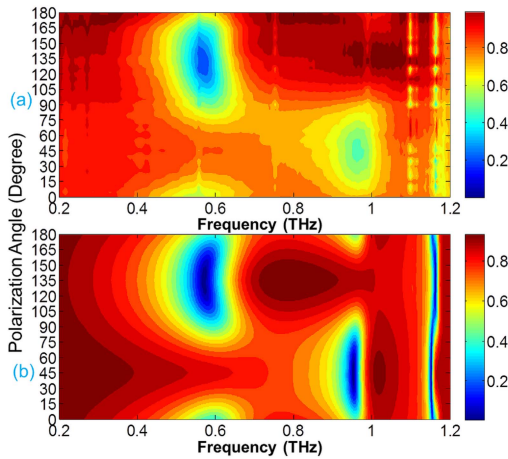


Fig. 2. (a) The measured transmission spectra of the FSS device. (b) The simulated transmission spectra of the FSS device.

proposed FSS sample (pFSSs), which make it good for THz transmittance measurement.

III. EXPERIMENTAL SETUP AND DEVICE MEASUREMENT

A THz-time domain spectroscopy (TDS) system is applied to characterize the pFSSs. The setup is similar to our previous work [8], where a homemade GaAs:O [9] bow-tie antenna is pumped by an 800 nm femto-second (fs) laser to generate THz radiations. The wire-grid polarizer used in the measurement set-up is tilted at a small angle to incident THz wave to minimize the multi-reflection.

To obtain the polarization dependence of pFSSs, the transmission spectra is measured with the intervals of 5 degrees in experimental measurement. Fig. 2(a) shows the measured pFSSs transmission spectra. The pFSSs transmission properties are also simulated with the full-wave electromagnetic (EM) simulation software: CST Microwave Studio. (Note: Drude model of the copper is used for simulation, where $\omega_p = 1.12e16$ (rad/s), $\omega_\tau = 2.2e12$ (1/s) [10]). Both the simulated and experimental results are shown in Fig. 2, which exhibits good consistency although with some differences in the polarization dependence, Such consistency is more clear in the region from 0.4 to 1 THz.

The difference between the simulated and experimental results is mainly due to three folds: 1) the pFSSs is not perfectly perpendicular to the THz beam during the measurement; 2) in simulation, the FSS device size is assumed to be infinite, which means it is periodically expanded without limitation. However, the real pFSSs size is only 1 cm \times 1 cm, i.e., hence the boundary effect could not be neglected since the reflections of evanescent wave at the edge of the sample on the surface can make the resonate peak a little broader than the simulated one; 3) The transmission dip around 0.75 THz and 1.1 THz in Fig. 1(a) come from the vapor absorption.

IV. ANALYSIS AND DISCUSSION

As mentioned above, the measurement results prove that the FSS device has good polarization dependent characteristics.

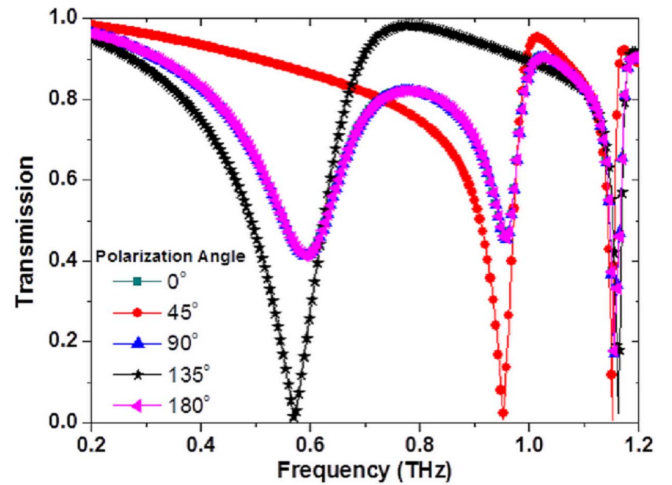


Fig. 3. The simulated transmission spectra of the FSS as a function of the incident polarization angle.

When the polarization angle of the FSS device is set to 135°, one could get a reflection resonance peak at 0.57 THz from the simulation, as shown in Fig. 2(b) and Fig. 3, and at 0.56 THz from the experiment, as shown in Fig. 2(a) respectively. This tiny difference is from the measurement deviation as mentioned in section III. In addition, when the polarization angle is changed to 45°, the resonant peak at 0.57 THz disappeared, and a new reflection resonance peak appeared at around 0.94 THz. For normal polarization angles (0, 90, 180 degrees.), the device has more than one resonant peaks in the range from 0.5 to 1 THz, and all these angles have the same transmission spectra, owing to the symmetry of proposed device.

For the non-bent-line structure, the FSS device is polarization independent, and it has only one resonance peak at 0.94 THz in the range of 0.1–1 THz. After adding the connecting bent-lines to the device, the congregated charges at the two near edges of the SRRs can be combined together. When the polarization angle is set to be 135°, the positive and negative charges at the near edges would cancel each other via the connections, as shown in Fig. 1(a). Therefore, there is no resonance peak at 0.94 THz, as shown in Fig. 3. However, the opposite charges in the two far edges of ELC resonators still exist, which makes the separation of charges become larger than the original. Thus a new resonant peak appears around 0.57 THz in the spectrum and its surface current is shown in Fig. 1 (c). When the polarization angle is set to be 45°, the charges at the near edges of those two ELC resonators had the same sign, which could enhance the original resonance result in a stronger resonance peak than the original one at 0.94 THz. Meanwhile, the charges at the far edges of those two ELC resonators also had the same sign, which could not induce resonance. Therefore there is no resonance peak at 0.57 THz in this case.

Furthermore, the transmission effect is also simulated with different the ELC resonator sizes. The resonant peak position moves toward lower frequency when increasing L_{ELC} or L_c for all polarization angles. It can be found that the position

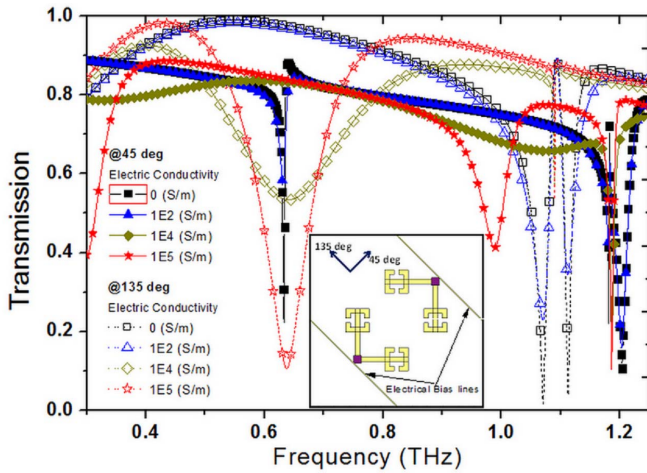


Fig. 4. The simulated THz wave transmissions of the designed device (inset) as a function of frequency at various conductivity of joint areas.

shift of the first resonance peak (around 0.57 THz, refer to Fig. 3) is more sensitive to L_c change, because the changes in L_c can induce tuning effect of the resonance effective length for nearly two times. Also, the second resonance peak (around 0.94 THz) can be modified by tuning L_{ELC} . One can suppose that a device with such two resonant peaks (peak position can be shifted by tuning L_{ELC} or L_c) can be used as polarization dependent channel switcher. For example, 135 degrees is for channel 1 and channel 2 is for 45 degrees, and 90 degrees is for dual-channel operation, etc.

The tunability of bent-lines can also be applied for active THz device fabrication. For example, two additional copper lines (width: $1\ \mu\text{m}$) can be designed as electrical bias lines and attached to the edge of the joint area of the bent-lines, the square as shown in purple in Fig. 4 (inset). By tuning the conductivity of the joint area one can switch the resonant peak of FSS. Fig. 4 shows the simulation results for such kind of active device, with the size of square area set to be $10\ \mu\text{m} \times 10\ \mu\text{m}$, the unit size of the designed active device of $220\ \mu\text{m}$, $L_c = 33\ \mu\text{m}$, $L_{ELC} = W_{ELC} = 30\ \mu\text{m}$, and the thicknesses of the PI substrate is $25\ \mu\text{m}$.

The most interesting thing for this active device is that the transmission of terahertz wave ($\sim 0.64\text{THz}$) decreases at 135° when we increasing the conductivity of the square area from 0 S/m to $1\text{E}5\ \text{S/m}$, whereas the transmission increase at 45° . Therefore the transmission/reflection rate can be controlled between the two perpendicular components of the incident THz wave just by modifying the conductivity of the square area on the turning point of the bent-line. Therefore a terahertz wave (especially for reflection mode) at any polarization angle can be obtained by combining two perpendicular polarization components (45° and 135° as mentioned above) under the modulation mode by such kind of active device. Normally, $1\text{E}5\ \text{S/m}$ is not easy to achieve, but this design is not difficult to realize by depositing thin film semiconductor on those joint areas [11] or creating cantilever legs bent structure for the square parts [12].

V. CONCLUSION

The scheme of applying FSS device to THz wave polarization dependent filtering is proposed in this letter. The FSS device is fabricated on a flexible PI substrate with a copper layer, and the polarization selective transmission is achieved successfully. At 45° polarization angle, the simulations show that the FSS device performed like a 4 ELC resonators without connecting bent-line. And at 135° polarization angle, a resonance peak appeared at 0.57 THz because of the offset of resonant charges via the bent-lines. Such characteristics of the device are verified by the experiment as well. Furthermore, the joint areas can be inserted into the FSS structure for an active frequency selection. The relation between the conductivity of the joint areas and the resonant peak position/strength is analyzed by the CST software. This feature is useful for the fabrication of narrow band polarization modulator.

ACKNOWLEDGMENT

The authors are grateful to Prof. K. T. Chan from The Chinese University of Hong Kong for continuous support of this letter.

REFERENCES

- [1] B. A. Munk, *Frequency Selective Surfaces: Theory and Design*. New York, NY, USA: Wiley, 2000.
- [2] M. E. MacDonald, A. Alexanian, R. A. York, Z. Popović, and E. N. Grossman, "Spectral transmittance of lossy printed resonant grid terahertz bandpass filters," *IEEE Trans. Microw. Theory Tech.*, vol. 48, no. 4, pp. 712–718, Apr. 2000.
- [3] J. C. Vardaxoglou, *Frequency Selective Surfaces*. New York, NY, USA: Wiley, 1997.
- [4] W. Withayachumnankul, *et al.*, "Sub-diffraction thin-film sensing with planar terahertz metamaterials," *Opt. Express*, vol. 20, no. 3, pp. 3345–3352, 2012.
- [5] D. Schurig, J. J. Mock, and D. R. Smith, "Electric-field-coupled resonators for negative permittivity metamaterials," *Appl. Phys. Lett.*, vol. 88, no. 4, pp. 041109-1–041109-3, 2006.
- [6] M. D. Rotaru and J. K. Sykulski, "Improved sensitivity of terahertz label free bio-sensing application through trapped-mode resonances in planar resonators," *IEEE Trans. Magn.*, vol. 47, no. 5, pp. 1026–1029, May 2011.
- [7] K. Aydin, I. Bulu, K. Guven, M. Kafesaki, C. M. Soukoulis, and E. Ozbay, "Investigation of magnetic resonances for different split-ring resonator parameters and designs," *New J. Phys.*, vol. 7, no. 1, p. 168, 2005.
- [8] S. Q. Du, *et al.*, "Vibrational frequencies of anti-diabetic drug studied by terahertz time-domain spectroscopy," *Appl. Phys. Lett.*, vol. 100, no. 14, pp. 143702-1–143702-4, 2012.
- [9] K. Chen, Y.-T. Li, M.-H. Yang, W. Y. Cheung, C.-L. Pan, and K. T. Chan "Comparison of continuous-wave terahertz wave generation and bias-field-dependent saturation in GaAs:O and LT-GaAs antennas," *Opt. Lett.*, vol. 34, no. 7, pp. 935–937, 2009.
- [10] M. A. Ordal, R. J. Bell, R. W. Alexander, Jr, L. L. Long, and M. R. Querry, "Optical properties of fourteen metals in the infrared and far infrared: Al, Co, Cu, Au, Fe, Pb, Mo, Ni, Pd, Pt, Ag, Ti, V, and W," *Appl. Opt.*, vol. 24, no. 24, pp. 4493–4499, 1985.
- [11] H.-T. Chen, *et al.*, "Experimental demonstration of frequency agile terahertz metamaterials," *Nature Photon.*, vol. 2, pp. 295–298, May 2008.
- [12] H. Tao, A. C. Strikwerda, K. Fan, W. J. Padilla, X. Zhang, and R. D. Averitt, "Reconfigurable terahertz metamaterials," *Phys. Rev. Lett.*, vol. 103, no. 14, pp. 147401-1–147401-4, 2009.